



Interacting coronae of two T Tauri stars

M. Massi¹, E. Ros^{2,1}, D. Böholtz³, K. M. Menten¹, J. Neidhöfer¹,
G. Torricelli-Ciamponi⁴, and J. Kerp⁵

- ¹ Max-Planck-Institut für Radioastronomie, Auf dem Hügel 69, D-53121 Bonn, Germany
e-mail: mmassi@mpi-fr-bonn.mpg.de
- ² Departament d'Astronomia i Astrofísica, Univ. de València, E-46100 Burjassot, Valencia, Spain
- ³ U.S. Naval Observatory, 3450 Massachusetts Ave, Washington DC 20392, USA
- ⁴ INAF, Osservatorio Astrofisico di Arcetri, Largo E. Fermi 5, I-50125 Firenze, Italy
- ⁵ Argelander-Institut für Astronomie, Univ. Bonn, Auf dem Hügel 71, D-53121 Bonn, Germany

Abstract. We present new high resolution VLBA+Effelsberg radio observations of V773 Tau A, a system of two T Tauri stars. Following the spatial and temporal evolution of flares, we try to define the structure of the interacting stellar coronae and to determine the energy of particles trapped in that structure.

Key words. Stars: flare – coronae – Stars: individual: V773 Tau – Radio continuum: stars

1. Introduction

The binary system V773 Tau A (Boden et al. 2007; Torres et al. 2012) shows outstanding magnetic activity, indicative of well developed magnetic coronae, demonstrated by radio and X-ray flares and the presence of large, cool, photospheric spots (Feigelson et al. 1994; Skinner et al. 1997; Tsuboi et al. 1998). A periodicity of 51.1 d, the same as the orbital one, has been discovered via long-term monitoring with the Effelsberg 100-m telescope (EB) in the radio flaring activity with large flares clustered around periastron passage (Massi et al. 2002). The orbit, with an eccentricity of $e = 0.27$ (Boden et al. 2007), results at apastron with a distance of 52 stellar radii ($1 R_* = 2$ solar radii) between the two stars, and at periastron

of 30 stellar radii. If the strong flaring activity at periastron is due to interacting coronae, then the magnetic structures should have sizes of at least 15 stellar radii. Observations at 90 GHz around periastron have monitored the onset and decay of a large flare and show that the rapid decay is consistent with continuous leakage of the emitting relativistic electrons from a magnetic structure of 10–20 stellar radii, similar to solar helmet streamers (Massi et al. 2006). Indeed VLBA+EB observations around apastron have resolved the radio emission into structures of $\sim 18 R_\odot$ (Massi et al. 2008). Here we present new multiepoch VLBA+EB observations aimed to spatially trace the flare evolution and polarized emission around periastron passage where the intensity of the flares is highest.

Send offprint requests to: M. Massi

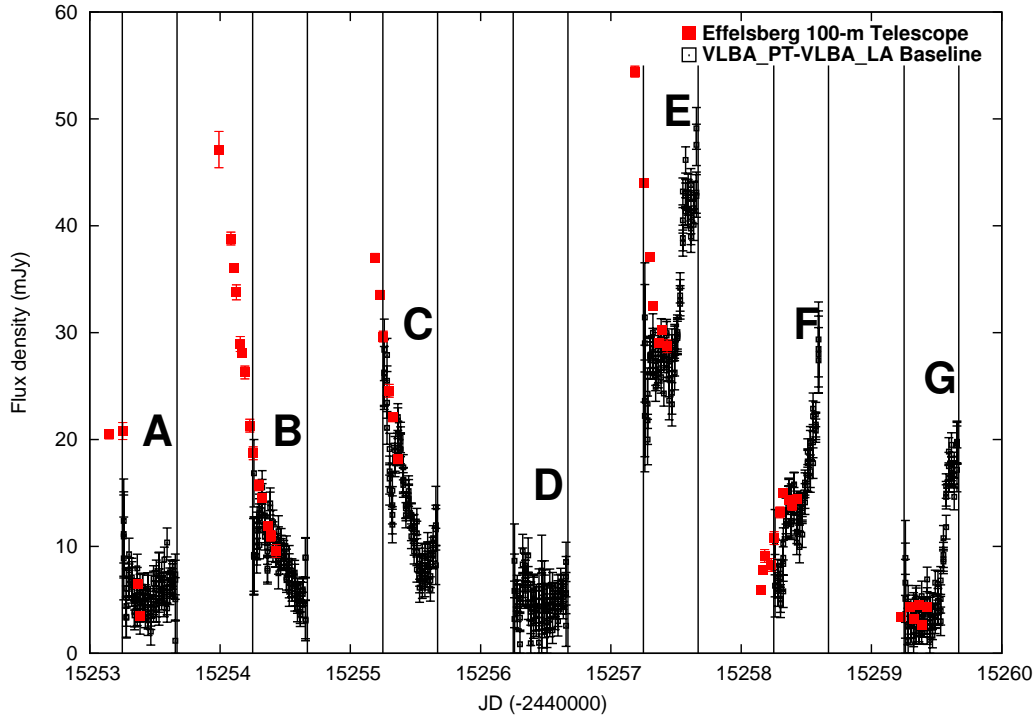


Fig. 1. Flux density as a function of time during VLBA+EB observations of 25 Feb.- 3 March 2010: There are 7 flares in 7 days. The Effelsberg 100-m telescope measured a flux density of 20 mJy before run A, that faded out during the run. Runs B and C observed the flares during their decay; runs F and G during their onset. For run E, during a flare decay a new flare occurred. The corresponding VLBA+EB images are shown in Fig. 2.

2. Observations and results

We observed V773 Tau A at 8.4 GHz over seven epochs from 2010 February 25 (run A) to 2010 March 3 (run G) with the ten 25 m antennas comprising the Very Long Baseline Array (VLBA) plus the Effelsberg (Germany) 100-m radio telescope. Figure 1 shows how the total flux density monitored with the 100 m Effelsberg telescope (resolution of 1.2 arc min at 8.4 GHz) overlaps with the visibility amplitude observed with the shortest baseline of the VLBA, Pie Town–Los Alamos (resolution of 31 mas at 8.4 GHz). This is an important constraint because it sets an upper limit of 4.5 AU for the largest magnetic structures, and it allowed us to monitor the flux-density-evolution of flares over the last 4 h of each run, where the source was no longer visible to the

Effelsberg telescope. In Fig. 2 two maps for each run are presented, the phase referenced and self-calibrated maps.

2.1. Flare decay

In the plots of Fig. 1, one can see that in each of the first three consecutive runs a total of three flares were observed by the VLBA at different phases of their decay: earlier in run C, more advanced in B, and through quiescence in A. In run D the emission remained at a low quiescent level for the entire 10 h. The VLBA+EB images in Fig. 2 allow us to follow the spatial evolution of the flares. The earlier phase of the flare in C, shown in Fig. 1, is also traceable spatially in Fig. 2 by the presence of a large structure around the secondary star. The fading flares in B and A show still emission between

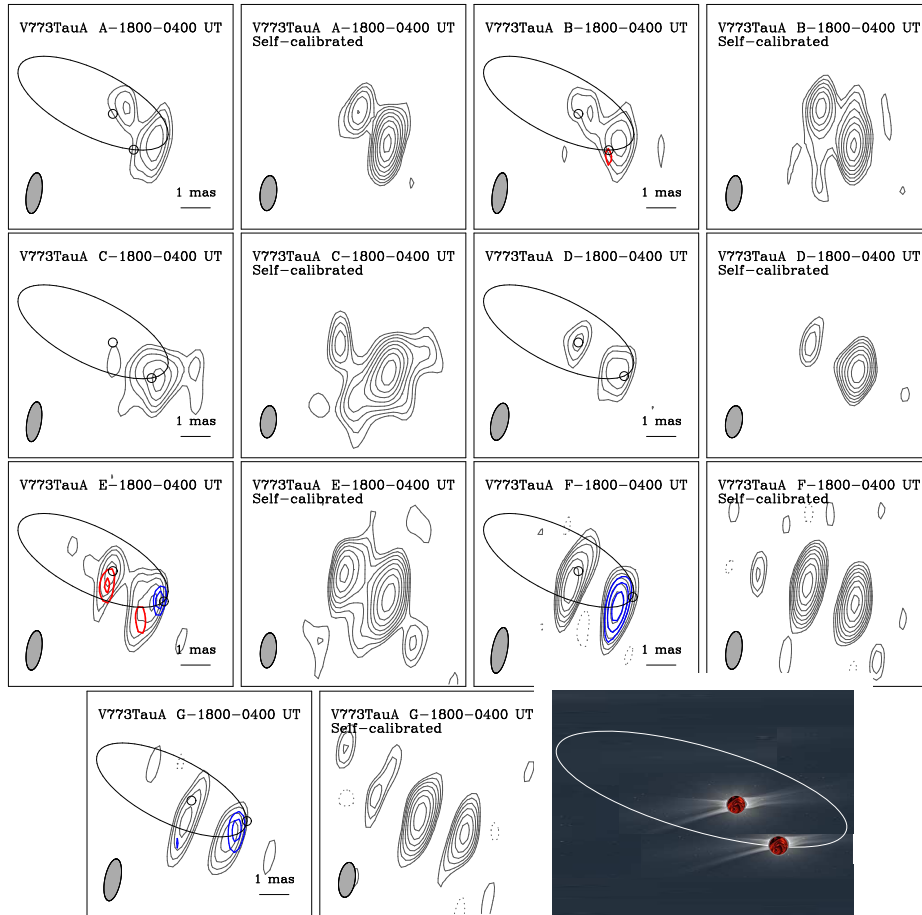


Fig. 2. Images of seven consecutive 8.4 GHz VLBA+EB observations of V773 Tau A. For each run (A,B,C,D,E,F, and G) two maps are presented, the phase-referenced (overlaid is the orbit of the binary stellar system) and the self-calibrated maps. The position of the secondary star is set according to the hybrid orbital solution for V773 Tau A by Boden et al. (2007). The circle of $4 R_*$ centered at each star's position indicates a symmetrical corona of an average size of $3 R_*$ (the stellar radius corresponds to 0.07 mas at 132.8 pc distance (Torres et al. 2012)). The restoring beam is shown in the bottom left corner of each map; it is on average of 0.5×1.4 mas for phase-referenced maps and 0.5×1.2 for self-calibrated maps. Contour levels are $-1, 1, 1.4, 2, 2.8, 4, 5.6, 8, 11.3, 16$ times the 4σ level. For runs A,B,C,D,E,F,G a 4σ level corresponds respectively to $0.4, 0.5, 0.7, 0.4, 2.0, 0.6, 0.5$ mJy/beam for the phase-referenced maps, and to $0.2, 0.2, 0.2, 0.2, 0.6, 0.3, 0.2$ mJy/beam for the self-calibrated maps. The peak flux density in each of the maps is (from A to G): $1.6, 2.0, 2.8, 1.0, 7.5, 1.7, 1.9$ mJy/beam for the phase-referenced maps and $2.1, 2.6, 3.3, 2.0, 7.6, 4.1, 2.2$ mJy/beam for the self-calibrated maps. Circularly polarized emission (traced in colour) is associated with the secondary star in E, F, and G with V/I equal to $-4.3\% \pm 0.4\%$, $-8.0\% \pm 0.3\%$ and $-8.0\% \pm 0.6\%$ and also to the primary in E, with opposite polarization sense and V/I of $4.0\% \pm 0.4\%$. Bottom right: sketch of the stellar system (out of scale). This image uses the photo of the solar corona by Miloslav Druckmuller (Brno Univ. of Technology), Peter Aniol, Vojtech Rusin in <http://www.zam.fme.vutbr.cz/druk/Eclipse/Ecl12008m/0-info.htm> reproduced with permission.

the two stars, in B more intense than in A. comes only from the two stars. We divided the In run D the quiescent emission lasting 10 hr

data in blocks of 3-4 h each and performed gaussian fits. Whereas the emission of the extended structure in run C has a fast temporal and spatial evolution, on the contrary the unresolved emission around the two stars in run D remains very stable. This confirms the scenario of electrons not well trapped in the streamers as in the coronal loops beneath. Leakage of relativistic electrons into free space from the tops of the streamers (Massi et al. 2006) is consistent with the rapid drop of interbinary emission of run C. On the other hand, leakage at the bottom of the streamer – through the helmet – by electrons penetrating into the coronal loop structure beneath should give rise to a long lasting emission as that observed in run D. In fact, for synchrotron losses the following relationship holds between magnetic field intensity B (in Gauss), electron Lorentz factor γ , and observed decay (τ , in hours) (Blumenthal & Gould 1970): $\gamma B^2 = \frac{2.2 \times 10^5}{\tau_{\text{synchrotron}}}$. In addition, the emission of each relativistic electron with Lorentz factor γ moving in a magnetic field B is centered around a peak spectral frequency ν_0 (Ginzburg & Syrovatski 1965) of $\nu_0 = 1.8 \times 10^6 B \gamma^2$ Hz. This implies that, to reproduce the observed emission at $\nu = 8.4$ GHz, electrons must exist for which the following relationship holds: $B \gamma^2 = 4.7 \times 10^3$. Therefore, for run D and a $\tau_{\text{synchrotron}} = 10$ hr, it results $B=47$ G and $\gamma=10$. On the other hand a magnetic dipole field, with $B(R_*)$ at the stellar surface, attains the intensity of 47 G at a distance $H/R_* = [B(R_*)/47]^{1/3}$. For $B_* = 2$ kG (Carroll et al. 2012), this would imply $H=3.5 R_* = 0.24$ mas for the structure around the stars in D.

2.2. Flare onset

In the last three days we picked up three new flares during their onset. Whereas in runs F and G the flares begin from the quiescent level, in

run E the flare emerges from a high level of emission remaining from a previous flare monitored by the Effelsberg telescope, 1.6 h before the VLBA observations. Circularly polarized emission is present in all three E, F, and G maps relative to a flare onset and always associated to the secondary star. In run E, emission of opposite sense of polarization is associated with the primary star.

3. Conclusion and discussion

The observed flaring rate of about 1 flare per day (Fig. 1) and the stellar rotation of 2 days are consistent with rather asymmetric extended structures like solar streamers on both hemispheres of the star interacting with each other during stellar rotation. Our high spatial resolution observations are revealing exciting features during the onset and during the decay of flares, indicating short-lasting emission in extended structures and long-lasting, low-level emission around the stars. Gaussian model fitting of the radio structures is in progress.

References

- Blumenthal, G. R., & Gould, R. J. 1970, *Rev. Mod. Phys.*, 42, 237
- Boden, A. F., et al. 2007, *ApJ*, 670, 1214
- Carroll, T. A., Strassmeier, K. G., Rice, J. B., & Kuentler, A. 2012, arXiv:1211.2720
- Feigelson, E. D., et al. 1994, *ApJ*, 432, 373
- Ginzburg, V. L., & Syrovatski, S. I. 1965 *ARA&A*, 3, 297
- Massi, M., Menten, K., & Neidhöfer J. 2002, *A&A*, 382, 152
- Massi, M., et al. 2006, *A&A*, 453, 959
- Massi, M., et al. 2008, *A&A*, 480, 489
- Skinner, S. L., Guedel, M., Koyama, K., & Yamauchi, S. 1997, *ApJ*, 486, 886
- Torres, R. M., et al. 2012, *ApJ*, 747, 18
- Tsuboi, Y., et al., 1998, *ApJ*, 503, 894